

Engineering

Industrial & Management Engineering fields

Okayama University

Year 1997

Analysis of electric-fluid analogy of
pressure transmission through an
electro-rheological-fluid in annuli

Yutaka Tanaka
Okayama University

Akio Gofuku
Okayama University

Keiji Nakamura
Okayama University

This paper is posted at eScholarship@OUDIR : Okayama University Digital Information
Repository.

<http://escholarship.lib.okayama-u.ac.jp/industrial-engineering/95>

Analysis of Electric-Fluid Analogy of Pressure Transmission through an Electro-Rheological-Fluid in Annuli

Yutaka Tanaka*, Akio Gofuku*, and Keiji Nakamura**

* Department of Systems Engineering, Okayama University
3-1-1 Tsushima-Naka, Okayama 700, Japan

** Graduate School of Engineering, Okayama University
3-1-1 Tsushima-Naka, Okayama 700, Japan

Present address: Nakashima Propeller Co.

ABSTRACT

This paper describes a technique to predict the transient response of pressure control device using electro-rheological fluid (ERF) by an electric-flow analogy. The inertance is calculated from the theoretical equation. The resistance and additional voltage source by the ER effect are derived theoretically by assuming the flow in the electrode annuli of the pressure control device as a flow of the Bingham fluid. The capacitance is determined to compare the time-responses of pressures by the prediction based on a model with the results of a simple experiment. The predictions of transient flow using the determined parameters of the model are in qualitatively good agreement with the experimental results.

1 Introduction

The authors have developed an artificial hand equipped with several flexible fingers. The three dimensional deformation of them is controlled by their internal pressure. The previous studies[1,2] investigate the construction of the finger, deformation control by air pressure, and installation of compact tactile sensors. However, the deformation control system by air pressure needs an air compressor, which results in a large and heavy control system and the generation of air discharge noise. In consideration of the demerits of the use of air compressor, the authors are now investigating the feasibility of the usage of electro-rheological fluids (ERFs) as pressure control fluids.

In order to design a finger and examine pressure control techniques, the transient responses of the fingers should be predicted by numerical simulation in addition to examining them by experiments. This study proposes

a modeling of ERF flow field by an electric-fluid analogy[3]. In the electric-fluid analogy, a flow field is modeled by an electric circuit based on the analogy of basic transient equations between the flow field and the electric circuit. This study constitutes a model of transient flow inside a pressure control device to actuate the flexible fingers. The parameters of resistance and additional voltage source which appear in the model of the pressure control device are derived by assuming that the flow inside electrode annuli can be approximated as a flow of the Bingham fluid. The inertance is calculated as a fluid inertia. Because the capacitance is greatly influenced by the amount of tiny air voids in the fluid, the capacitance is estimated from the results of a simple experiment.

This paper firstly summarizes a technique to control the pressure of flexible fingers in Sec. 2. Section 3 introduces the electric-fluid analogy[3]. Section 4 firstly describes the derivation of the parameters of resistance and additional voltage source. Then, the estimation of capacitance is described. Section 5 describes a transient model of pressure control device and discusses the prediction results. Finally, the results of this study are summarized in Conclusions.

2 Pressure control device of electro-rheological-fluid

Two kinds of ERF are used in this study. The one (ERF 1) is the mixture of the dispersoid, Diaion (commercial name) having the effective diameter of 0.18 μ m, and the dispersion medium, Trimex T-08 (tri-methylhexil-tritrate) which has good affinity with the dispersoid. The weight fraction of the dispersion is set at 30 and 40 %. Another ERF (ERF 2) is SR-1 which is a standard ERF of Japanese Society of Rheology[4].

Figure 1 shows the schematic of the principle of pressure control using an ERF. The electrodes shown in the left of the figure are made by connecting two annuli shown in Fig. 2. The ERF is allowed to flow in the direction of the arrow in the annular region (electrode

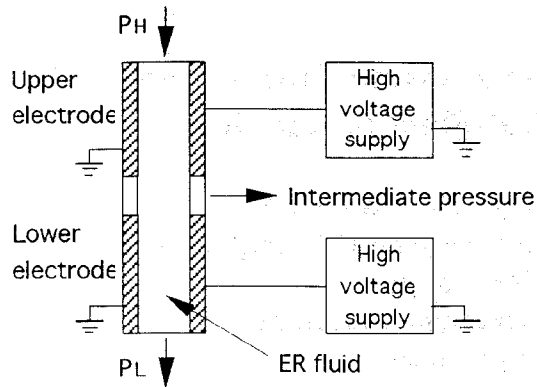


Fig 1. Principle of pressure control by ERF.

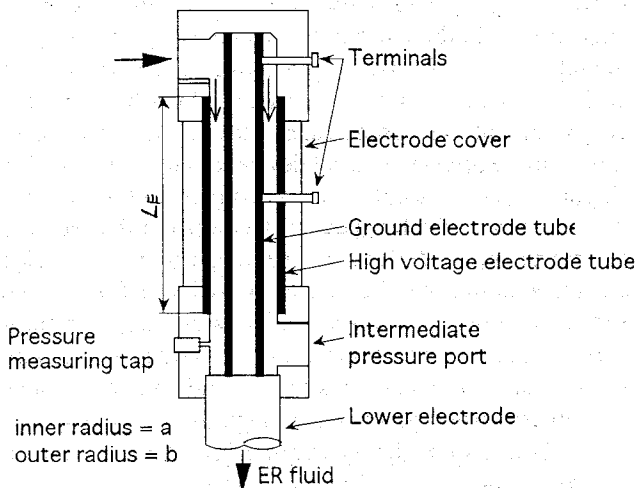


Fig 2. Schematic of electrode.

gap 1mm and electrode length L_E) between the inner cylindrical electrode (ground pole) of outer diameter 8 mm and the outer one (positive pole) of inner diameter 10 mm. The apparent viscosity of ERF increases by the application of electric field. This means that we can control pressure drop in ERF flow by changing the amplitude of electric field. Suppose that the high voltages applied to the upper and lower electrodes are controlled in such a way that the total pressure drop in the upper and lower electrodes is constant. In this case, the intermediate pressure can be controlled between inlet pressure of the upper electrode and outlet pressure of the lower electrode.

The authors have developed a high voltage control system and examine the characteristics of pressure control using the two types of ER fluids. High voltage is supplied to an electrode through high voltage circuits whose input voltages from two high voltage power supplies are controlled by the use of solid state relays (S.S.R.). Because high speed voltage change is required in the measurement of pressure response characteristics, high slewing rate and amplification type high voltage power supplies are used. Although ERF can be fed by a pump,

any existing pump damages ERF, which causes pressure fluctuation and introduces experimental errors. Hence, the ERF pressured by air in a confined vessel is supplied to the pressure control device in order to minimize the possible pressure fluctuation.

3 Electric-fluid analogy

In the electric-fluid analogy[3], a flow field is modeled as the electric circuit as shown in Fig. 3 by the analogy of basic transient equations between flow field and electric circuit. The pressure P and flow rate Q correspond to electric potential difference E and current I , respectively. The resistance R , inertance L , and capacitance C for the flow field are respectively defined as

$$P = RQ, \quad (1)$$

$$P = L \frac{dQ}{dt}, \text{ and} \quad (2)$$

$$P = \frac{1}{C} \int Q dt. \quad (3)$$

The inertance is caused by the inertia of ERF. If the dispersed particles and tiny voids in the ERF is assumed to be small compared with the flow width and they distribute uniformly in the fluid, the pressure P is given by

$$P = \frac{dQ}{dt} \int \frac{\rho dx}{A} = L \frac{dQ}{dt} \quad (4)$$

where A , ρ , and dx are cross sectional area of flow, density of ERF, and minute flow length, respectively. In addition, if the density is constant through the flow length L_E , the inertance L is given by

$$L = \int \frac{\rho dx}{A} = \frac{\rho L_E}{A} \quad (5)$$

On the other hand, the capacitance is a parameter in relation with the compressibility of fluid. If it is assumed that (i) the deformation of dispersed particles are neglected, (ii) the particles and tiny voids distribute

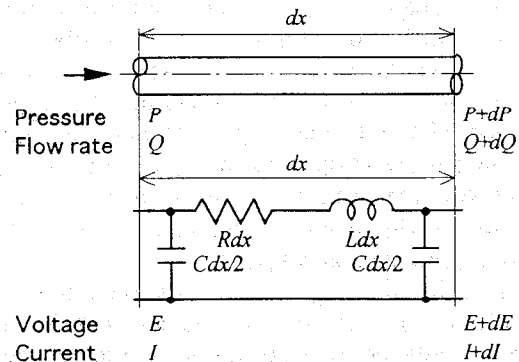


Fig 3. Model of flow field by electric-fluid analogy.

uniformly, (iii) cross sectional area of flow A is constant through the flow length L_E , and (iv) the pressure is time-invariant (p_0), the capacitance is given as

$$C = \frac{AL_E}{K' p_0} \quad (6)$$

where K' is an apparant bulk modulus of elasticity. However, K' decreases greatly with an increase in the total of tiny voids mixed in ERF. It also decreases by the small expansion of pipe due to the increase of fluid pressure. The capacitance is estimated by the simple experiment which will be described in Sec. 4 considering the difficulty of measurements of tiny voids mixed in ERF.

The resistance and additional voltage source are derived by assuming that the flow field in the coaxial double cylindrical pipes is expressed as one of Bingham type as will be described in Sec. 4.

4 Electric-fluid analogy of electro-rheological-fluid

4.1 Theoretical analysis of flow field of ERF

The following assumptions are made in this theoretical analysis of flow field of ERF: i) the fluid is incompressible and laminar, ii) viscous coefficient μ and fluid density ρ are constants invariable to time and place, and iii) the energy of motion of the fluid is negligible. Under the assumptions, the shear stress and the equation of motion for one dimensional flow in the axial direction x are respectively expressed as

$$\tau = \mu \frac{\partial u}{\partial r} \pm \tau_E(E) \quad (7)$$

$$\rho \frac{\partial u}{\partial t} + \frac{1}{r} \frac{\partial(r\tau)}{\partial r} = \frac{\partial p}{\partial x} \quad (8)$$

where $\tau_E(E)$, u , r , p , a , and b are shear stress induced at the electric field intensity E , axial flow velocity, radial distance measured from the pipe center axis, pressure, and outer and inner radii of the annular flow field, respectively. In Eq. (7), '+' is used when momentum is transported in the + r direction, while '-' when transport is in the - r direction.

If $\tau_E(E) = 0$, the non-steady solution for Eq. (8) is given by Von W. Muller[5]. Because the solution for Eq. (8) in the case of $\tau_E(E) \neq 0$ becomes a complicated one, it is assumed that the flow field is steady and its radial flow profile is represented by the Bingham plastic flow. Equation (8) is integrated twice with respect to the annular flow region considering that the annular flow field has the plug flow region where the radial velocity gradient becomes zero. The obtained velocity expression u is integrated over r and the flow rate Q in the annular region is derived. Following the long derivation procedure by

Fredrickson[5], the relationship between the volume flow rate $Q = \int_b^a 2\pi r u dr$ and the pressure gradient $P = -\partial p / \partial r \approx (p - p_L) / L_E$ is obtained as

$$Q = \frac{\pi a^4 P}{8\mu} \left\{ 1 - \kappa^4 - 2\sigma_o \sigma_i (1 - \kappa^2) - \frac{4}{3} (1 + \kappa^3) T_E + \frac{1}{3} (2\sigma_o - T_E)^3 T_E \right\} \quad (9)$$

where $T_E = 2\tau_E(E)/(Pa)$, σ_o , σ_i , L_E and p_L denote dimensionless limiting induced shear stress, dimensionless outer and inner radius of the plug flow region, pipe length and pressure at pipe outlet. At present, these derivation can be easily performed by using the mathematical software "Maple V". The σ_o and σ_i have the following relationship.

$$\sigma_i = \sigma_o - T_E \quad (10)$$

When we use dimensionless velocity defined by $\phi = 2\mu u / (Pa^2)$, the velocity distribution is expressed as follows[5]:

$$\phi_i = -T_E(\sigma - \kappa) - (\sigma^2 - \kappa^2) / 2 + \sigma_o \sigma_i \log(\sigma / \kappa) \quad \text{for inner flow region } (\kappa \leq \sigma \leq \sigma_i)$$

$$\phi = \phi_i(\sigma_i) = \phi_o(\sigma_o) \quad \text{for flat flow region } (\sigma_i \leq \sigma \leq \sigma_o)$$

$$\phi_o = -T_E(1 - \sigma) - (1 - \sigma^2) / 2 + \sigma_o \sigma_i \log(\sigma) \quad \text{for flat flow region } (\sigma_o \leq \sigma \leq 1) \quad (11)$$

The variables σ_o and σ_i are determined by the boundary conditions that the velocity profiles of the outer plug flow and inner regions are smoothly connected to each other.

The application of Eq. (9) to an actual flow field is not easy because Eq. (9) is apparently a fourth order equation with respect to the variable T_E . From this fact, Eq. (9) is simplified by assuming that the arithmetic mean between σ_i and σ_o is equal to the geometrical mean between them. Then, we have

$$Q = \frac{\pi a^4 P}{8\mu} \left\{ 1 - \kappa^4 - (\kappa^2 - 1)^2 / \ln(1/\kappa) \right\} - \frac{\pi a^3 \tau_E}{12\mu} \left[-4(1 + \kappa^3) + \left\{ 2(1 - \kappa^2) / \ln(1/\kappa) \right\}^{3/2} \right] \quad (12)$$

The shear stress τ_E which is a parameter of Eqs. (9) and (12) is expressed as a function of applied electric field E from experimental results of the relationship between pressure difference and flow rate when E is changed. The function is obtained as

$$\tau_E = 0.60 E^2 \quad (13)$$

When the non-steady state solution by Von W.

Muller[5] is integrated over the annular pipe section and the result is combined with the steady state solution (Eq. (8)), the transient flow rate in an electrode is approximated by only considering the first order root ξ_i of Bessel function as[7]

$$\varepsilon \frac{\partial Q}{\partial t} + Q = \frac{H(p - p_L)}{L_E} - K\tau_E(E) \quad (14)$$

where

$$\begin{aligned} \varepsilon &= \rho / (\mu \xi_1^2) \\ K &= \frac{\pi a^3}{12\mu} \left[4(1 + \kappa^3) - \left\{ 2(1 - \kappa^2) / \ln(1/\kappa) \right\}^{3/2} \right] \\ H &= \frac{\pi a}{8\mu} \left\{ 1 - \kappa^4 - (\kappa^2 - 1)^2 / \ln(1/\kappa) \right\} \end{aligned} \quad (15)$$

If the flow is assumed to have the flat velocity distribution, the time constant ε is approximated by

$$\varepsilon = \frac{\rho a^2}{8\mu} \left\{ 1 + \kappa^2 - \frac{4\kappa^2 \ln(1/\kappa)}{1 - \kappa^2} \right\} \quad (16)$$

Next, the validity of the theoretical expression is discussed by examining how accurately the flow rate Q and the intermediate pressure p calculated by the simplified relationship Eq. (12) coincide with the experimental data.

Figure 4 shows the relationship between the ratio of the statically applied electric field and the intermediate pressure when the sum of the electric fields applied to the electrodes was changed successively as $E_s = 0.8, 1.6,$ and 2.0 kV/mm and the maximum pressure is kept constant ($p_H = 0.392$ MPa). Figure 5 represents the flow rate changes under the conditions identical to those in Fig. 4. These figures show both the experimental results and the theoretical calculation results obtained by applying the empirical equation (13) for τ_E to the steady state ones (14) and (15). In this calculation, the pressure drops in the central pipe between two electrodes and in the ports connecting the central pipe and the annular pipes are neglected. From the figures, the theoretical expression is concluded to explain quantitatively the experimental results not only for the pressure but also for the flow rate.

Finally, Eq. (12) is transformed to be the form of $P = RQ + E$ to model the flow field of an electrode by the electric-fluid analogy. Then, we obtain the resistance and additional voltage source for an electrode of length L_E as

$$R = \frac{8\mu L_E}{\pi a^4} \left\{ \frac{1}{(1 - \kappa^4) - (1 - \kappa^2)^2 / \ln(1/\kappa)} \right\} \quad (17)$$

$$E = \frac{\pi a^3 R}{\mu} \left\{ \frac{1}{3}(1 + \kappa^3) - \frac{2}{3} \left(\frac{1 - \kappa^2}{2 \ln(1/\kappa)} \right)^{3/2} \right\} \tau_E \quad (18)$$

4.2 Estimation of capacitance

The capacitance is estimated by a simple experiment. Figure 5 shows the configuration of the experiment. The ERF in the vessel is pressurized to be p_A by air pressure. The ERF is initially flowing out to the reservoir through the open valve and the annulus. The length of the pipe is $L_{11} = 50$ mm, $L_{12} = 300$ mm, and $L_{13} = 50$ mm. In this initial flow condition, the valve is abruptly closed and the time responses of the pressures $p_{11}, p_{12},$ and p_{13} are measured by a digital oscilloscope.

A transient model of the experiment is constituted by the electric-flow analogy and the capacitance is estimated by comparing the time responses between prediction by the model and experimental data. Figure 6 shows the transient model, where the annulus is divided into three parts at the pressure measurement points. The electric potentials and currents $E_{11}, E_{12}, E_{13}, i_{11}, i_{12},$ and i_{13} in Fig. 6 correspond to pressures and flow rates $p_{11}, p_{12}, p_{13}, Q_{11}, Q_{12},$ and Q_{13} , respectively. The abrupt closure of the valve corresponds to the step-wise change of electric potential E_{11} from E_A to 0.

By establishing and manipulating the transient equations in the model, the relations among $E_{11}, E_{12},$ and E_{13} are finally obtained as

$$\begin{bmatrix} E_{11} & i_{11} \end{bmatrix} = \mathbf{F}_{11} \mathbf{F}_{14} \begin{bmatrix} E_{12} & i_{12} \end{bmatrix}^T \quad (10)$$

$$\begin{bmatrix} E_{11} & i_{11} \end{bmatrix} = \mathbf{F}_{11} \mathbf{F}_{12} \mathbf{F}_{13} \begin{bmatrix} E_{13} & i_{13} \end{bmatrix}^T \quad (11)$$

where

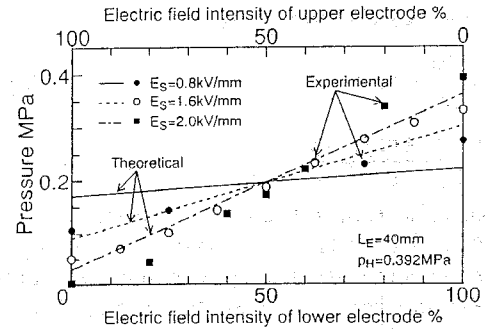


Fig. 4. Intermediate pressure vs. electric field.

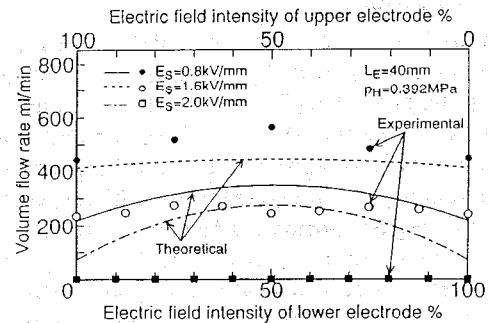


Fig. 5. Flow rate change vs. electric field.

$$\begin{aligned}
 F_{11} &= \left[\begin{array}{cc} 1 + \frac{(R_{11} + sL_{11})sC_{11}}{2} & R_{11} + sL_{11} \\ sC_{11} \left(1 + \frac{(R_{11} + sL_{11})sC_{11}}{4} \right) & 1 + \frac{(R_{11} + sL_{11})sC_{11}}{2} \end{array} \right] \\
 F_{12} &= \left[\begin{array}{cc} 1 + \frac{(R_{12} + sL_{12})sC_{12}}{2} & R_{12} + sL_{12} \\ sC_{12} \left(1 + \frac{(R_{12} + sL_{12})sC_{12}}{4} \right) & 1 + \frac{(R_{12} + sL_{12})sC_{12}}{2} \end{array} \right] \\
 F_{13} &= \left[\begin{array}{cc} \frac{sC_{13}}{2} + \frac{1}{R_{13} + sL_{13}} & 0 \\ \frac{1}{R_{13} + sL_{13}} & 1 \end{array} \right] \\
 F_{14} &= \left[\begin{array}{cc} \frac{sC_{12}}{2} + \frac{1}{Y_{12} + Y_{13}} & 0 \\ \frac{1}{Y_{12} + Y_{13}} & 1 \end{array} \right] \\
 Y_{12} &= \frac{1}{R_{12} + sL_{12}} \\
 Y_{13} &= \frac{sC_{12}}{2} + \frac{sC_{13}}{2} + \frac{1}{R_{13} + sL_{13}}
 \end{aligned}
 \tag{12}$$

are 3.09×10^{-12} , 5.44×10^{-12} , and 1.37×10^{-11} [Pa s²/m⁴] for ERF 1 (30%wt), ERF 1 (40%wt), and ERF 2 (40%wt), respectively. The estimated capacitance of ERF 1 (40%wt) is smaller than that of ERF 1 (30%wt). This estimated results qualitatively coincide with the theoretical expression by Eq. (6) such that the capacitance is in inverse proportion to the bulk modulus of elasticity

5 Prediction of transient response of pressure control device

5.1 Model to predict transient response

A model to predict transient response of the flow in electrode annuli of the pressure control device is constituted as shown in Fig. 8. The left part of the electric circuit corresponds to the upper electrode, while right part lower electrode. The voltage source E_A corresponds to the pressure at the inlet of the upper electrode. The voltage sources e_1 and e_2 correspond to the ER effect by the application of electrical field to ERF.

The basic differential equations for the electric circuit are formulated by the Kirchoff's laws as

$$i_1 = i_2 + i_3 \tag{13}$$

$$i_3 = i_4 + i_5 \tag{14}$$

$$i_5 = i_6 + i_7 \tag{15}$$

$$E_A = \frac{2}{C} \int i_2 dt \tag{16}$$

$$\frac{2}{C} \int i_2 dt = e_1(t) + Ri_3 + L \frac{di_3}{dt} + \frac{1}{C} \int i_4 dt \tag{17}$$

$$\frac{1}{C} \int i_4 dt = e_2(t) + Ri_5 + L \frac{di_5}{dt} + \frac{2}{C} \int i_6 dt \tag{18}$$

and

$$\frac{2}{C} \int i_6 dt = R_0 i_7 \tag{19}$$

The estimated capacitances of the two types of ERF

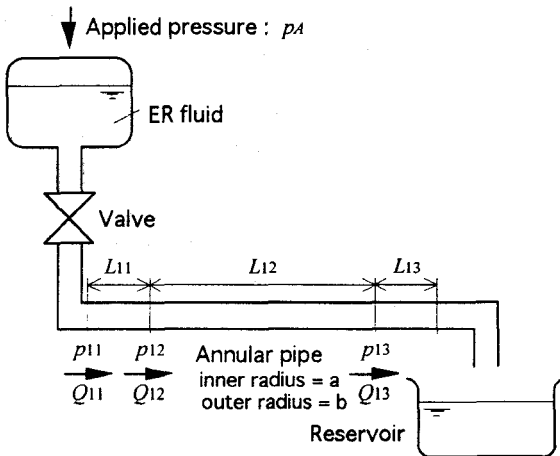


Fig 6. Experiment to estimate capacitance.

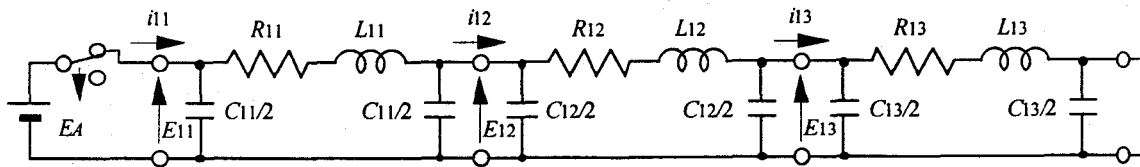


Fig 7. Model for the experiment to estimate capacitance.

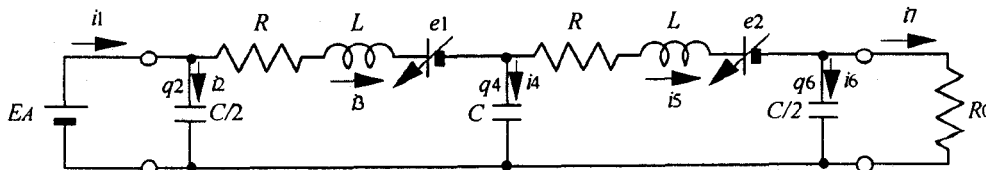


Fig 8. Model of pressure control device to predict transient response.

By solving the Eqs. (13) to (19) considering the initial conditions for the variable $q_6 = \int i_6 dt$, we obtain

$$\begin{aligned}
& E_A - e_1(t) - e_2(t) - CR \frac{de_2(t)}{dt} - LC \frac{d^2 e_2(t)}{dt^2} \\
&= L^2 C \frac{d^4 q_6}{dt^4} + \left(2LCR + \frac{2L^2}{R_0} \right) \frac{d^3 q_6}{dt^3} \\
&+ \left(4L + 4 \frac{LR}{R_0} + CR^2 \right) \frac{d^2 q_6}{dt^2} + \left(4R + \frac{4L}{CR_0} + \frac{2R^2}{R_0} \right) \frac{dq_6}{dt} \\
&+ \left(\frac{2}{C} + \frac{4R}{R_0} \right) q_6 \quad (21)
\end{aligned}$$

Because a time delay is observed from the step-wise change of applied voltage to the appearance of ER effect, the time responses of e_1 and e_2 are approximated by a first-order function with delay time constant T . Considering $e_1(0) = e_s$, $e_2(0) = 0$, and the initial conditions, the Laplace transformation of q_6 is obtained as

$$\begin{aligned}
Q &= \frac{c_1 s^3 + c_2 s^2 + c_3 s + c_4}{c_1 s^4 + c_2 s^3 + c_3 s^2 + c_4 s + c_5} c_6 \\
&+ \frac{1}{c_1 s^4 + c_2 s^3 + c_3 s^2 + c_4 s + c_5} \\
&\times \left\{ \frac{E_A}{s} + \frac{LCe_s}{T} - \frac{e_s}{1+sT} \left(T + \frac{1}{s} + CR + LCs \right) \right\} \quad (26)
\end{aligned}$$

where

$$\left. \begin{aligned}
c_1 &= L^2 C \\
c_2 &= 2LCR + \frac{2L^2}{R_0} \\
c_3 &= 4L + \frac{4LR}{R_0} + CR^2 \\
c_4 &= 4R + \frac{4L}{CR_0} + \frac{2R^2}{R_0} \\
c_5 &= \frac{CR_0}{2} \frac{E_A - e_1(0) - e_2(0)}{2R + R_0}
\end{aligned} \right\} \quad (27)$$

The time response E_{22} is obtained by substituting the inverse Laplace transformation of Eq. (26) into the following equation

$$\begin{aligned}
E_{22} &= e_2(t) + \left(\frac{2R}{CR_0} + \frac{2}{C} \right) q_6 + \left(R + \frac{2L}{CR_0} \right) \frac{dq_6}{dt} \\
&+ L \frac{d^2 q_6}{dt^2} \quad (28)
\end{aligned}$$

5.2 Prediction of transient flow inside electrode annuli

As an example of predicting the transient responses of electrodes, Fig. 9 shows the time responses of the

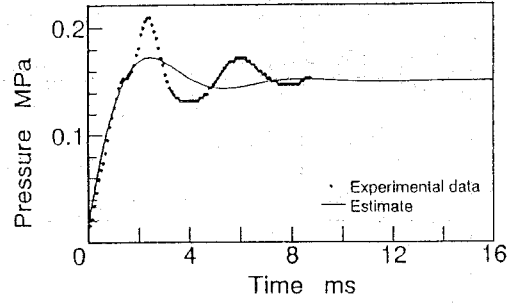


Fig 9. Experiment to estimate capacitance.

intermediate pressure by the calculation (solid line) and experiment (dotted line) using ERF 2. Although the overshooting wave form is underestimated, the period of fluctuation by the prediction agrees well with that in the experimental results.

6 Conclusions

This paper describes a technique to predict the transient response of pressure control device using ERF by the electric-flow analogy. The results obtained in this study is summarized in the following:

(i) The resistance and additional voltage source by the ER effect derived theoretically under the assumption of Bingham flow explain quantitatively the steady state flow in the electrodes of pressure control device.

(ii) The estimated capacitances by fitting the transient prediction by a model based on the electric-fluid analogy to a simple experiment coincide qualitatively well with the theoretical expression.

(iii) The predictions of transient flow by the constituted model are in qualitatively good agreement with the experimental results.

References

- [1] Tanaka, Y., *Mechatronics*, 3, (1), 59-75 (1993).
- [2] Tanaka, Y., Gofuku, A., and Fujino, Y., *Proc. 1996 4th Int. Workshop on Advanced Motion Control*, Tsu, Japan, March 1996, Vol. 2, 723-728 (1996).
- [3] Sawaragi, Y., et al., *Trans. Soc. Instrument and Control Engineers*, 2, (1), 63 (1966). (in Japanese)
- [4] Ishino, Y., Maruyama, T., Osaki T., Endo S., Saito T., and Goshima N., *Proc. 41th Workshop on Rheology*, 112-115 (1993). (in Japanese)
- [5] Muller, V. M., *Z.F. angew. Math. und Mech.*, 6, (16), 227-238 (1936).
- [6] Fredrickson, A. G. and Bird, R. B., *Industrial and Engineering Chemistry*, 50, (3), 347-352 (1958).
- [7] Tanaka, Y. and Gofuku, A., *Mechatronics*, to be appeared.